haematologica
Journal of the Ferrata Storti Foundation

COUP-TFII regulates hemoglobin switching by activating the BCL11A-XL repressor Lin28B and directly binding δ and β globin promoters in fetal *versus* adult erythroid cells

by Carlotta Frigo, Valentina Pastori, Gianluca Zambanini, Martina Fabiano, Sajeela Ahmed, Elisabetta Citterio, Claudio Cantù and Antonella Ellena Ronchi

Received: June 17, 2025.
Accepted: November 17, 2025.

Citation: Carlotta Frigo, Valentina Pastori, Gianluca Zambanini, Martina Fabiano, Sajeela Ahmed, Elisabetta Citterio, Claudio Cantù and Antonella Ellena Ronchi. COUP-TFII regulates hemoglobin switching by activating the BCL11A-XL repressor Lin28B and directly binding δ and β globin promoters in fetal versus adult erythroid cells.
Haematologica. 2025 Nov 27. doi: 10.3324/haematol.2025.288485 [Epub ahead of print]

COUP-TFII regulates hemoglobin switching by activating the BCL11A-XL repressor Lin28B and directly binding δ and β globin promoters in fetal *versus* adult erythroid cells

Carlotta Frigo[1*], Valentina Pastori[1*], Gianluca Zambanini[2, 3, 4*], Martina Fabiano[1], Sajeela Ahmed[1], Elisabetta Citterio[1,5], Claudio Cantù[2,3,6 ^] and Antonella Ellena Ronchi[1^]

[1]Dipartimento di Biotecnologie e Bioscienze, Università degli Studi di Milano-Bicocca, Milan, Italy.

[2]Wallenberg Centre for Molecular Medicine, Linköping University, Linköping, Sweden.

[3]Division of Molecular Medicine and Virology, Department of Biomedical and Clinical Sciences, Faculty of Medicine and Health Sciences, Linköping University, Linköping, Sweden.

[4]Present address: Max-Planck-Institut für molekulare Genetik, Berlin, Germany.

[5]Department of Life Science, Health, and Health Professions, LINK Campus University, Rome, Italy.

[6]Science for Life Laboratory – SciLifeLab, Linköping University, 58185 Linköping, Sweden

[*]Co-First Authors

[^]Co-Corresponding Authors:

Antonella Ellena Ronchi, Dipartimento di Biotecnologie e Bioscienze, Università degli Studi di Milano-Bicocca, P.za Scienza 2, 20126 Milan, Italy

email: antonella.ronchi@unimib.it

Claudio Cantù, Linköping University, Department of Biomedical and Clinical Sciences, 581 83, Linköping, Sweden

email: claudio.cantu@liu.se

Authors's contribution: C.F., V.P., G.Z. performed experiments, data analysis and data interpretation. M.F., S.A. helped with experimental work. E.C. interpreted data and wrote the manuscript. C.C. and A.E.R. conceived the experiments, interpreted data and wrote the manuscript.

Running heads: COUP-TFII, LIN28B and BCL11A-XL interplay

DATA Sharing Agreement: address all correspondence to C.C. and A.E.R. Data are available at Array express E-MTAB-14720, under private access.

Funding: This work was supported by the European Union's Horizon 2020 Research and Innovation Program under the Marie Skłodowska Curie grant agreement No. 813091 (A.E.R.), by MUR - Ministero dell'Università e della Ricerca (PRIN: 2021-NAZ-0253) (A.E.R.) and by the European Union - NextGenerationEU through the Italian Ministry of University and Research under PNRR - M4C2-I1.3 Project PE_00000019 "HEAL ITALIA" to A.E.R. (H43C22000830006), from the Swedish Research Council, Vetenskapsrådet [2021-03075 and 2023-01898], Linköping University and LiU/RÖ-Cancer, Cancerfonden [CAN 2018/542 and 21 1572 Pj], and Additional Ventures (USA) [SVRF2021-1048003] to C.C. The views and opinions expressed are those of the authors only and do not necessarily reflect those of the European Union or the European Commission. Neither the European Union nor the European Commission can be held responsible for them. C.C. is a Wallenberg Molecular Medicine (WCMM) fellow and receives generous financial support from the Knut and Alice Wallenberg Foundation. The computations and data handling were enabled by resources provided by the National Supercomputer Centre (NSC), funded by Linköping University; Peter Münger at the National Supercomputer Centre is acknowledged for assistance concerning technical and implementational aspects in making the codes run on the Sigma resource. The sequencing was carried out by the Cantù laboratory at the molecular biology unit of Linköping University's core facility.

Acknowledgements: We thank Giulia Lavizzari for drawing the model in Figure 4, Yukio Nakamura for the gift of HUDEPs cells, Sergio Ottolenghi and John Strouboulis for reading, discussion and suggestions.

Disclosure of interest: No interests to declare

ABSTRACT

The reactivation of fetal globin genes is the most promising treatment for β-hemoglobinopathies. This implies the reversal of the naturally occurring hemoglobin switching. Here, we show that expression of the orphan nuclear receptor COUP-TFII in adult HUDEP2 erythroid precursor cells activates γ-globin (HbF) at the expense of β-adult globin by specific occupation of the "adult" δ-β-region within the β-locus. Notably, although COUP-TFII and the main γ-globin repressor BCL11A-XL share a similar DNA binding consensus and a large number of chromatin targets, including the locus control region of the β-locus itself, they bind differentially to the γ and β promoters, eliciting an opposite transcriptional outcome. In addition, we find that COUP-TFII activates LinN28B, a known post-transcriptional repressor of BCL11A-XL. Our work identifies a molecular mechanism that could be leveraged to increase γ-globin levels in patients affected by β-hemoglobinopathies.

INTRODUCTION

The switching from fetal (HbF) to adult (HbB) globin expression is a crucial event during development and the possibility of reverting it represents a concrete therapeutic option for patients suffering from β-hemoglobinopathies (1, 2).

In this perspective, efforts to reactivate fetal γ-globin to cure β-hemoglobinopathies have primarily focused on targeting HbF repressors, with BCL11A-XL being one of the most important(3-7).

Erythroid-specific inactivation of BCL11A-XL has been proven to be an effective therapeutic strategy(1), emphasizing the importance of uncovering mechanisms and players that influence developmental globin genes expression. On the other hand, the molecular understanding of HbF activation is still largely unknown.

In this direction, we recently demonstrated that the orphan nuclear receptor COUP-TFII/NR2F2, which is physiologically expressed during mouse development in cells of yolk sac origin (8), is capable of reactivating fetal globin when re-expressed in adult cells (including human Sardinian β^{039}-thalassemic cells), thus overcoming the repressive environment dictated by the presence of the full set of fetal globin repressors. However, its molecular mechanism of action remains largely unexplored.

Here, to understand the mechanistic basis of the ability of Coup-TFII to promote embryo/fetal erythropoiesis and to partially revert globins expression in adult cells, we undertook a genome-wide analysis of Coup-TFII binding in HUDEP cells(9). These cells, immortalized from human cord blood, offer the unique advantage to model globins gene regulation in fetal versus adult erythropoietic environments: HUDEP1 uniquely express fetal γ-globin, whereas HUDEP2 express adult β-globin and the full set of γ-globin repressors, including BCL11A-XL. Since COUP-TFII recognizes on DNA the GGTCA motif of nuclear receptors (10-12), which is virtually identical to that of BCL11A-XL (13) (14), HUDEP2 cells allow to test whether the ability of COUP-TFII to overcome γ-globin repression relies on its direct competition with BCL11A-XL for the occupancy of the same DNA sequences within the β-locus. In addition, the comparison of CUT&RUN profile in HUDEP1 and HUDEP2 offers the possibility to assess chromatin genomic redistribution of COUP-TFII in fetal-like versus adult-like cells and to identify targets -besides globin loci- relevant for controlling hemoglobin switching.

We discovered that COUP-TFII reactivates γ-globin in HUDEP2, where it occupies the adult δ and β promoters. Moreover, COUP-TFII likely contributes to the maintenance of the fetal-like globins expression profile by directly activating the γ-globin inducer LIN28B, a post-transcriptional BCL11A-XL repressor (10, 11).

The discovery of these novel mechanisms of COUP-TFII-mediated γ activation offers a new perspective for developing strategies to treat β-hemoglobinopathies.

METHODS

Single cell analysis

Single-cell RNA sequencing data were obtained from Popescu et al.(12) (E-MTAB-7407) via the Human developmental cell atlas and from Ranzoni et al., 2021(13) (E-MTAB-9067). For fetal livers, further data processing and analysis were performed using Scanpy (version 1.10.4) and Numpy (version 2.0.2). Cells with fewer than 200 detected genes were excluded, and cells with mitochondrial DNA content exceeding 5% were also removed to reduce potential biases from stressed or dying cells. After normalization, fetal liver datasets were annotated with Celltypist (v1.6.3), applying the pre-trained "Pan_Fetal_Human.pkl" model to ensure consistency across analyses. For yolk sac (YS) data, no additional pre-processing steps were applied and Cell type annotation followed the original authors' classification. The results were visualized using UMAP embeddings.

Cells lines

HUDEP1 and HUDEP2 cells were grown according to standard protocols(9). Detailed media and conditions are described in Table 1.

Constructs

The Nr2f2 murine cDNA was cloned into the IRES-EmeraldGFP (eGFP) pHR SIN BX IR/EMW lentiviral vector(8). psPAX2 and pMD2.GVSVG packaging plasmids were used to produce Lentiviral pseudo-particles in HEK293T cells (lentiweb.com).

Lentiviral transduction

72h post HEK293T cells transfection recombinant virus particles were collected and titrated on K562 cells. A MOI of 20-30 was use to transduce HUDEP1 and HUDEP2 cells. The percentage of infected cells (scored as eGFP+ cells) used in the experiments was ≥ 75% (Supplemental Figure 1).

RNA isolation and RTqPCR

Total RNA was purified with TRIzol Reagent (Euroclone) and retrotranscribed (High Capacity cDNA Reverse Transcription Kit, Applied Biosystem). Real time analysis was performed on a StepOneTM instrument (Applied Biosystems) by using SsoAdvanced™ Universal SYBR® Green Supermix (Bio-Rad). Primers are listed in Table 3.

Western Blot

Total and nuclear extracts were prepared according to standard procedures. Protein extracts (5–10 µg/lane) were resolved by SDS/PAGE in a 10-15% acrylamide gel and blotted onto Hybond-ECL Nitrocellulose membrane (GE healthcare). Membranes were blocked, incubated with the appropriate antibodies and after washing, ECL reagent (Millipore) was used for detection. Antibodies are listed in Table 2.

CUT&RUN

CUT&RUN-LoV-U was performed as described in Zambanini et al. (14). Per each sample 500,000 cells were harvested (HUDEP1/2 untransduced or transduced with the COUPT-FII vector). Cells were washed three times with nuclear extraction buffer and the nuclei were bound to Magnetic ConA Agarose beads. Samples were incubated with antibodies overnight. Antibody in excess was washed and the sample where incubated with pAG-MNase 30 minutes at 4 °C. pAG-MNase in excess wash washed and digestion was initiated on ice using CaCl2 [2 mM] and stopped in STOP buffer after 30 minutes sharp. Digestion buffer was collected and the beads were resuspended in Urea STOP buffer for DNA elution for 1 hour at 4° C. Digestion buffer of each sample was mixed with the corresponding DNA elution. DNA was bound to beads, the supernatant was discarded and beads were washed two times in Ethanol 80%. DNA was eluted in Tris-HCl and the procedure was repeated twice

adding new beads. Libraries preparation and data processing are detailed in Supplemental Methods.

Electrophoretic mobility shift assay (EMSA)

Nuclear extracts from COS7 cells transfected either with a BCL11A-XL-myc or a COUP-TFII-Flag vector were prepared according to ref. (15). The oligonucleotide sequence, from the ApoA1 enhancer: FW: 5' ACTGAACCCTTGACCCTGCCCT, REV: 5' AGGGCAGGGTCAAGGGTTCAGT. 32P-labeled DNA oligonucleotide probe was incubated for binding with 1-3 µg of nuclear extracts (NE) for 20 min. at room temperature in a buffer containing 5% glycerol, 50mM NaCl, 20mM Tris pH7.9, 0.5mM EDTA, 5mM MgCl, 1mM DTT, 100ng/ml poly(dI-dC), 50ng/ml BSA and 0.05% PFA in a 15µl final reaction mixture. Protein-DNA complexes were then separated on a 5% polyacrylamide gel (29:1 acrylamide/bisacrylamide ratio) and visualized by autoradiography. BCL11A-XL and COUP-TFII bands were univocally identified by using anti-myc (Ab32 Abcam) and anti-Flag (F7425Sigma-Aldrich) antibodies.

RESULTS

COUP-TFII expression in early human erythropoiesis

In E11.5 mouse embryonic liver, *Coup-TFII* is expressed in Erythroid-Myeloid-Progenitors (EMPs) and decreases as these cells undergo erythroid maturation (8). To understand whether this expression pattern is conserved in human erythropoiesis, we analyzed three single-cell RNAseq datasets, representative of three different timepoints: 4-7 post conception weeks (PCW) yolk sac(12), 7-17 PCW fetal liver(12) and 17-22 PCW fetal liver(13) (Figure 1). The 4-7 PCW yolk sac dataset by Popescu et al. (12) identifies two discrete cell populations expressing Coup-TFII (left panel). The first population is annotated as endothelium and expresses high levels of Coup-TFII and little globins. The second population, annotated as megakaryocyte-erythroid-mast cell progenitors (MEMP), co-expresses Coup-TFII and globins (predominantly HBG2).

Discrete cell populations co-expressing Coup-TFII and globin genes (Coup-TFII^{+}globins^{+}) are also identified in fetal liver by two independent datasets, representative of consecutive

developmental stages (middle and right panels). In both fetal liver datasets, a Coup-TFII^{+}globins^{+} population is identified as endothelium. At 7-17 PWC, an additional population called "vascular smooth muscle cell (VSMC) pericytes" is identified. The genes commonly expressed at this stage by these two Coup-TFII^{+}globins^{+} populations, are associated with Diamond-Blackfan anemia (DBA) by the Orphanet database of rare diseases (https://maayanlab.cloud/Enrichr/enrich?dataset=608a66f9e8a7bd75e308bd91e8ed9024). DBA is a rare congenital aplastic anemia with erythroblastopenia affecting very early erythroid progenitors. This observation is consistent with early-erythroid features.

In all three datasets, Coup-TFII expression becomes undetectable in highly hemoglobinized cells, compatible with Coup-TFII decline during erythroid differentiation, as we previously observed in mouse(8). The "endothelium", "vascular smooth muscle cell (VSMC) pericytes", and "MEMP" annotations are in line with the thought common ontogenic origin of these cell types. (16-18).

COUP-TFII and BCL11A-XL interplay

In adult cells, including Thalassemic $\beta^{0}39$ cells, COUP-TFII re-expression induces γ-globin at the expense of adult β-globin (8). Here, to study the molecular mechanism of COUP-TFII-mediated γ activation in adult cells, we re-expressed it in adult-like HUDEP2 (expressing adult β-globin) and in fetal-like HUDEP1 (expressing fetal γ-globin) cord blood- derived progenitors. In HUDEP2, COUP-TFII induces γ-globin both at the RNA (Figure 2A) and protein level (Figure 2B), as expected. The BCL11A-XL consensus site on DNA is identical to the canonical COUP-TFII binding motif (GGTCA, Figure 2C). On this basis, we hypothesized that COUP-TFII could directly compete with BCL11A-XL for its genomic occupancy at the γ-globin promoters(19). To test this hypothesis, we first checked for the ability of BCL11A-XL to bind *in vitro* in EMSA assays to a well-known COUP-TFII DNA consensus on the ApoAI enhancer(20). As shown in Figure 2D, this probe is indeed bound by both proteins, each univocally identified by supershift with specific antibodies. We then mapped the genome-wide occupancy of COUP-TFII in HUDEP2 by CUT&RUN and we compared it with that of BCL11A-XL, published by Liu et al.(19). As a control, we also performed COUP-TFII CUT&RUN in fetal-like HUDEP1 cells, which do not express BCL11A-XL and express high levels of γ-globin. To this end, we generated both HUDEP1 and HUDEP2 cells expressing a tagged version of COUP-TFII (Suppl. Figures 1 and 2).

The comparison of CUT&RUN datasets for BCL11A-XL and COUP-TFII in HUDEP2 cells revealed a substantial number of common peaks (Figure 2E-F), as well as protein-specific genomic binding sites. Of interest in this context, the top differentially expressed genes (DEGs) associated with peaks generated by COUP-TFII (HUDEP1 and HUDEP2 results merged) are similar to the genes perturbed by BCL11A knockout in mice (https://maayanlab.cloud/Enrichr/enrich?dataset=bfd73c13b56ba7bbecd7a75c3e725f5c), supporting the idea that these two proteins could regulate the same genes in opposite direction by competing for DNA occupancy of the same sequences (Figure 2G).

To specifically address COUP-TFII-BCL11A-XL interplay in globins regulation, we mapped their binding within the β-locus in HUDEP2 (Figure 2H), taking advantage of data published by Liu et al.(19). This analysis revealed that the two proteins share common peaks at the locus control region (LCR). In particular, COUP-TFII is recruited to the DNAseI hypersensitive sites (DHS), where it prominently occupies the β-HS3 (Figure 2H). Surprisingly, COUP-TFII does not bind to the GGTCA sequences within the γ-promoters, which are the targets of BCL11A-XL (19). Instead, COUP-TFII occupies the "adult" δ- and β-globin promoters (Figure 2H), likely interfering with their interaction with the LCR.

COUP-TFII binding to the globin loci

To deepen our analysis, we generated two additional replicates of the COUP-TFII CUT&RUN experiment using an additional COUP-TFII antibody and we considered only the peaks present in at least three out of the four replicates (Supplemental Figure 2). This analysis returns a Coup-TFII binding profile at the β-locus, shown in Figure 3A, which is superimposable to the one in Figure2H. Further footprinting mapping confirmed COUP-TFII binding at the δ and β promoters (Figure 3B). This region is a known target of natural deletional hereditary persistence of fetal hemoglobin, (HPFH)(21) and of artificial deletions created to mimic HPFH phenotype (Figure 3C).

In HUDEP1 cells, which are devoid of BCL11A-XL and express γ-globin levels about 40 times higher than in HUDEP2 cells (calculated as ratio on GAPDH), COUP-TFII still binds to the LCR region (Figure 3D). However, COUP-TFII is not detected at the "adult" promoters, revealing its ability to rearrange its occupancy within the locus during development. In these same cells, COUP-TFII expression increases ε-globin but not the already high and likely saturated γ-globin expression (Figure 3E).

Notably, COUP-TFII, while activating γ-globin, in parallel, it reduces β-globin transcription (Figure 2A). This occurs in both HUDEP2 and HUDEP1 cells, where β-globin is expressed at marginal levels (Figure 3E).

Finally, at the α-globin locus, COUP-TFII shows a similar occupancy pattern in HUDEP1 and HUDEP2 and favors embryonic ζ-globin expression when compared to α-globin (Supplemental Figure 3).

COUP-TFII contributes to the maintenance of the fetal-like environment by activating Lin28B

Our CUT&RUN dataset allowed us to search for potential direct regulation by COUP-TFII of additional genes involved in hemoglobin switching. We focused on BCl11A-XL and Lin28B, selectively expressed in adult-like HUDEP2 and in fetal-like HUDEP1 cells, respectively. As shown in Figure 4A, in HUDEP2 cells, COUP-TFII occupies the +55Kb DNAseI hypersensitive site within the known *BCL11A* erythroid enhancer(22) and weakly represses its transcription in differentiation conditions. In HUDEP1, we could not detect COUP-TFII peaks within the *BCL11A* locus, which has a closed chromatin conformation (ATACseq data from ref. (23)).

HUDEP1 cells express *LIN28B,* an oncofetal gene(24) encoding for an RNA binding protein capable of activating γ-globin in adult cells(10) by interfering with BCL11A-XL translation(11). In these cells, we show that COUP-TFII activates LIN28B, increasing both its RNA and protein levels (Figure 4B). In HUDEP2 cells, where the LIN28B locus is not accessible, COUP-TFII does not bind to the LIN28B locus (data from ref. (23)). Together, these data suggest that, depending on chromatin accessibility, COUP-TFII can contribute to the fetal-to-adult transition through cell-type selective occupancy at *BCL11A* and *LIN28B* loci, as we propose in Figure 4C.

DISCUSSION

Research aiming at reactivating fetal globin in patients suffering from β-hemoglobinopathies has so far focused exclusively on targeting γ-repressors. How γ-globin is activated in embryo/fetal cells remains largely unclear. We recently reported for the first time that Coup-TFII activates γ-globin at the expense of the adult β-globin gene in human normal and β-thalassemic cells(8).

In the present work, to understand how COUP-TFII overrides fetal globins repression in adult cells, partially restoring a fetal-like environment, we profiled its expression in early human development in scRNA dataset (Figure1) and we mapped its genomic occupancy by CUT&RUN in HUDEP1 (fetal-like, γ-expressing) and in HUDEP2 (adult-like, β-expressing) cells. HUDEP1 γ-expressing cells allow to model human fetal-like erythropoietic cells, hardly accessible for ethical and technical reasons. The comparison of COUP-TFII genomic occupancy in HUDEP1 and HUDEP2 cells revealed a significant genomic redistribution of COUP-TFII at the globins loci. COUP-TFII, when expressed in adult-like HUDEP2 cells, activates γ-globin both at the RNA and protein level (Figure2A-B), as expected on the basis of our previous results(8). Since COUP-TFII shares the same core DNA consensus with BCL11A-XL, the major γ-globin repressor in adult cells, (Figure 2C) and both proteins are able to recognize the same sequence *in vitro* (EMSA in Figure 2D), we compared their occupancy profile at the β-locus in detail (Figure 2H). Although the two proteins share a large number of genomic targets (Figure 2F-G), they also show significant differences. In both HUDEP1 and HUDEP2 COUP-TFII bind to the LCR, suggesting that it could participate into the transcription complexes assembled at the LCR that coordinate the sequential activation of globin genes transcription during development(25). However, surprisingly, COUP-TFII does not bind to the GGTCA sequences within the γ-promoters, which are the targets of BCL11A-XL (19). Instead, COUP-TFII occupies the "adult" δ- and β-globin promoters (Figure2H). In this scenario, we hypothesize that the presence of COUP-TFII at δ and β promoters could hinder/weaken their interaction with the LCR. This mechanism would lead to γ-globin activation at the expense of β-globin, as observed in Figure 2A, thereby overcoming the γ-globin silencing imposed by the concerted action of fetal repressors, including BCL11A-XL(26-28). The observation that Coup-TFII, while activating embryo/fetal globins, also reduces β expression (Figure2A) is consistent with our previous data obtained in β^{039} Thalassemia erythroid cultures from CD34+ cells (8). This finding suggests that reactivating COUP-TFII in adult cells may be a viable strategy to increase γ-globin also in sickle cell disease, while simultaneously inhibiting the intracellular accumulation of defective β^{S} chains. The potential clinical relevance of this observation in quantitative terms will require further investigation in appropriate cellular and *in vivo* HBS models.

Why COUP-TFII occupancy at the adult region is not detected in HUDEP1 cells is not clear. We think it may reflect different accessibility of this region, which is open only in

HUDEP2(23), allowing COUP-TFII recruitment to these positions. In HUDEP1, COUP-TFII expression increases ε-globin but not the already high and likely saturated γ-globin expression (Figure 3E).

By profiling Coup-TFII genome occupancy in fetal vs adult cells, we uncover an unexpected, multi-layered role of COUP-TFII in the differential regulation of globin genes expression. In HUDEP2 cells, Coup-TFII, beside binding to the δ and β promoters, it transcriptionally represses BCL11A-XL, by binding to its +55Kb enhancer (Figure 4A). However, in these cells, upon COUP-TFII expression, we failed to demonstrate a significant decrease of the BCL11A-XL protein. This result is unclear. We may speculate the existence during the fetal-to-adult switching, of some transient cell population -not captured by HUDEP1 and HUDEP2- in which COUP-TFII expression concurs to BCL11A-XL downregulation and thereby to the progressive establishment of an adult environment.

We could not detect COUP-TFII peaks within the closed *BCL11A* locus in HUDEP1 cells (ATACseq data from ref. (23)). In HUDEP1 cells, COUP-TFII promotes a fetal-like phenotype by transcriptionally activating Lin28B, a post-transcriptional repressor of BCL11A-XL(11) (Figure 4B).

Interestingly, we recently identified *LIN28B* as a target repressed by SOX6(29), a known γ-globin repressor that cooperates with BCL11A-XL (through protein-protein interaction) to the silencing of γ-globin(28).

Together, our data add a new layer to the complex regulatory network that controls the differential expression of globin genes. we suggest that the decline of COUP-TFII -together with the parallel increase in SOX6- during the fetal to adult transition state could contribute to hemoglobin switching through multiple mechanisms: direct regulation of the globin loci and modulation of the translation of BCL11A-XL through its posttranscriptional repressor LIN28B, as we propose in Figure 4C. As a note of caution, we wish to point out that this molecular model, derived from HUDEP cells, may not fully capture human hemoglobin switching *in vivo* and requires further validation in primary human cells around the switching time. Further *in vivo* studies will clarify whether changes in the fetal/adult globins ratio induced by Coup-TFII are clinically significant.

Overall, our present work contributes to understanding the molecular basis of COUP-TFII-mediated reactivation of γ-globin in adult cells within the β-locus and provides novel insights

into how COUP-TFII integrates in the complex network sustaining the embryo/fetal transcriptional milieu, favorable to γ-globin expression.

REFERENCES

1. Frangoul H, Altshuler D, Cappellini MD, et al. CRISPR-Cas9 Gene Editing for Sickle Cell Disease and beta-Thalassemia. N Engl J Med. 2021;384(3):252-260.
2. Dimitrievska M, Bansal D, Vitale M, et al. Revolutionising healing: Gene Editing's breakthrough against sickle cell disease. Blood Rev. 2024;65:101185.
3. Barbarani G, Labedz A, Stucchi S, et al. Physiological and Aberrant gamma-Globin Transcription During Development. Front Cell Dev Biol. 2021;9:640060.
4. Lettre G, Sankaran VG, Bezerra MA, et al. DNA polymorphisms at the BCL11A, HBS1L-MYB, and beta-globin loci associate with fetal hemoglobin levels and pain crises in sickle cell disease. Proc Natl Acad Si U S A. 2008;105(33):11869-11874.
5. Uda M, Galanello R, Sanna S, et al. Genome-wide association study shows BCL11A associated with persistent fetal hemoglobin and amelioration of the phenotype of beta-thalassemia. Proc Natl Acad Si U S A. 2008;105(5):1620-1625.
6. Menzel S, Garner C, Gut I, et al. A QTL influencing F cell production maps to a gene encoding a zinc-finger protein on chromosome 2p15. Nat Genet. 2007;39(10):1197-1199.
7. Menzel S, Thein SL. Genetic Modifiers of Fetal Haemoglobin in Sickle Cell Disease. Mol Diagn Ther. 2019;23(2):235-244.
8. Fugazza C, Barbarani G, Elangovan S, et al. The Coup-TFII orphan nuclear receptor is an activator of the gamma-globin gene. Haematologica. 2021;106(2):474-482.
9. Kurita R, Suda N, Sudo K, et al. Establishment of immortalized human erythroid progenitor cell lines able to produce enucleated red blood cells. PloS One. 2013;8(3):e59890.
10. Lee YT, de Vasconcellos JF, Yuan J, et al. LIN28B-mediated expression of fetal hemoglobin and production of fetal-like erythrocytes from adult human erythroblasts ex vivo. Blood. 2013;122(6):1034-1041.
11. Basak A, Munschauer M, Lareau CA, et al. Control of human hemoglobin switching by LIN28B-mediated regulation of BCL11A translation. Nat Genet. 2020;52(2):138-145.
12. Popescu DM, Botting RA, Stephenson E, et al. Decoding human fetal liver haematopoiesis. Nature. 2019;574(7778):365-371.
13. Ranzoni AM, Tangherloni A, Berest I, et al. Integrative Single-Cell RNA-Seq and ATAC-Seq Analysis of Human Developmental Hematopoiesis. Cell Stem Cell. 2021;28(3):472-487.e7.
14. Zambanini G, Nordin A, Jonasson M, et al. A new CUT&RUN low volume-urea (LoV-U) protocol optimized for transcriptional co-factors uncovers Wnt/beta-catenin tissue-specific genomic targets. Development. 2022;149(23)dev201124.
15. Schreiber E, Matthias P, Muller MM, et al. Rapid detection of octamer binding proteins with 'mini-extracts', prepared from a small number of cells. Nucleic Acids Res. 1989;17(15):6419.
16. Choi K, Kennedy M, Kazarov A, et al. A common precursor for hematopoietic and endothelial cells. Development. 1998;125(4):725-732.
17. Biben C, Weber TS, Potts KS, et al. In vivo clonal tracking reveals evidence of haemangioblast and haematomesoblast contribution to yolk sac haematopoiesis. Nat Commun. 2023;14(1):41.
18. Randolph LN, Castiglioni C, Tavian M, et al. Bloodhounds chasing the origin of blood cells. Trends Cell Biol. 2025:S0962-8924(25)00067-4.
19. Liu N, Hargreaves VV, Zhu Q, et al. Direct Promoter Repression by BCL11A Controls the Fetal to Adult Hemoglobin Switch. Cell. 2018;173(2):430-442.e17.
20. Park JI, Tsai SY, Tsai MJ. Molecular mechanism of chicken ovalbumin upstream promoter-transcription factor (COUP-TF) actions. Keio J Med. 2003;52(3):174-181.
21. Forget BG. Molecular basis of hereditary persistence of fetal hemoglobin. Ann N Y Acad Sci. 1998;850:38-44.
22. Bauer DE, Kamran SC, Lessard S, et al. An erythroid enhancer of BCL11A subject to genetic variation determines fetal hemoglobin level. Science. 2013;342(6155):253-257.

23. Huang P, Peslak SA, Ren R, et al. HIC2 controls developmental hemoglobin switching by repressing BCL11A transcription. Nat Genet. 2022;54(9):1417-1426.
24. Moss EG, Lee RC, Ambros V. The cold shock domain protein LIN-28 controls developmental timing in C. elegans and is regulated by the lin-4 RNA. Cell. 1997;88(5):637-646.
25. Gurumurthy A, Yu DT, Stees JR, et al. Super-enhancer mediated regulation of adult beta-globin gene expression: the role of eRNA and Integrator. Nucleic Acids Res. 2021;49(3):1383-1396.
26. Khandros E, Blobel GA. Elevating fetal hemoglobin: recently discovered regulators and mechanisms. Blood. 2024;144(8):845-852.
27. Masuda T, Wang X, Maeda M, et al. Transcription factors LRF and BCL11A independently repress expression of fetal hemoglobin. Science. 2016;351(6270):285-289.
28. Xu J, Sankaran VG, Ni M, et al. Transcriptional silencing of {gamma}-globin by BCL11A involves long-range interactions and cooperation with SOX6. Genes Dev. 2010;24(8):783-798.
29. Pastori V, Zambanini G, Citterio E, et al. Transcriptional repression of the oncofetal LIN28B gene by the transcription factor SOX6. Sci Rep. 2024;14(1):10287.
30. Nordin A, Zambanini G, Pagella P, et al. The CUT&RUN suspect list of problematic regions of the genome. Genome Biol. 2023;24(1):185.
31. Teytelman L, Thurtle DM, Rine J, et al. Highly expressed loci are vulnerable to misleading ChIP localization of multiple unrelated proteins. Proc Natl Acad Sci U S A. 2013;110(46):18602-18607.
32. Kountouris P, Lederer CW, Fanis P, et al. IthaGenes: an interactive database for haemoglobin variations and epidemiology. PloS One. 2014;9(7):e103020.

Table1: HUDEP cells growing media

Cell line		MEDIUM	Supplements
HUDEP proliferation		IMDM	0.2% HSA (Human Serum Albumin) 0.1% Lipid Mixture 300 µg/mL transferrin 10 µg/mL insulin 100 µM sodium pyruvate 2 U/mL EPO (Erythropoietin) 100 ng/mL SCF (Stem Cell Factor) 1 µM dexamethasone 2 µg/mL doxycycline
HUDEP differentiation (72h)		IMDM	3% HSA (Human Serum Albumin) 0.1% Lipid Mixture 1000 µg/mL transferrin 10 µg/mL insulin 100 µM sodium pyruvate 10 U/mL EPO (Erythropoietin) 2% FBS (Fetal Bovine Serum)

Table 2: list of antibodies and reagents

Antibodies and reagents	Cat n°	Manufacturer
Anti-FLAG	F7425	Sigma-Aldrich
Anti-Coup CUTandRUN A	ABIN6928040	
Anti-Coup CUTandRUN B and WB	ab41859	Abcam
Anti Lin28B	4196	Cell Signaling
Anti U2AF	U4758	Sigma-Aldrich
Anti Vinculin	AB129002	Abcam
Anti HbG	AB283313	Abcam
rIgG	PP64	Millipore
Phosphate-buffered saline (PBS)	ECB4004L	Euroclone
Fetal Bovine Serum (FBS)	F7524	Sigma-Aldrich
L-glutamine	ECB3000D	Euroclone
Penicillin-Streptomycin	ECB3001D	Euroclone
High Capacity cDNA RT Kit	4368814	Applied Biosystems
SsoAdvanced Universal SYBR® Green	1725274	Bio-Rad
IMDM medium	P04-20250	PAN
HUMAN SERUM ALBUMIN	P06-27100	PAN
rh SCF	11343325	ImmunoTools
rh EPO	11344795	ImmunoTools
dexamethasone	D4902	Sigma-Aldrich
doxycicline	D9891	Sigma-Aldrich
Lipid mixture	L0288	Sigma-Aldrich
Sodium pyruvate	P5280	Sigma-Aldrich
insulin	I6634	Sigma-Aldrich
transferrin	T1147	Sigma-Aldrich

Table 3: list of RTqPCR primers

Primers used for RT-PCR		
GENE	**F/R**	**Sequence (5'-3')**
GAPDH	**F**	ACGGATTTGGTCGTATTGGG
	R	TGATTTTGGAGGGATCTCGC
HBA	**F**	GAGGCCCTGGAGAGGATGTTCC
	R	ACAGCGCGTTGGGCATGTCGTC
HBB	**F**	TACATTTGCTTCTGACACAAC
	R	ACAGATCCCCAAAGGAC
HBG	**F**	CTTCAAGCTCCTGGGAAATGT
	R	GCAGAATAAAGCCTATC TTGAAAG
HBE	**F**	GCCTGTGGAGCAAGATGAAT
	R	GCGGGCTTGAGGTTGT
LIN28B	**F**	GCGCATGGGATTTGGATTCA
	R	ACTTCCTAAACAGGGGCTCC
HBZ	**F**	TCTGACCAAGACTGAGAGA
	R	TTGAAGTTGACCGGGTCCAC

FIGURE LEGENDS

Figure 1: co-expression of COUP-TFII and γ-globin in human early embryonic yolk sac and fetal liver

(A) UMAPs from single-cell RNA-seq data of the 4-7 PCW yolk sac (from ref. (12), left), 7-17 PCW fetal liver (from ref. (17), middle), and 17-22 PCW fetal liver (from ref. (13), right). COUP-TFII-expressing cells are highlighted according to the color key scale flanking each panel. **(B)** Cell type annotations for COUP-TFII positive clusters are shown for each dataset. **(C)** Dot plots displaying co-expression of COUP-TFII and globin genes across identified cell types in each dataset (rectangles). Circle size represents the fraction of cells expressing each gene, and color intensity reflects gene expression levels. MEMP: megakaryocyte-erythroid-mast cell progenitor; VSMC: vascular smooth muscle cell.

Figure 2: COUP-TFII reactivates embryo/fetal globin genes in HUDEP2 cells

A) RT-qPCR analysis of mRNA levels for the indicated globin genes in HUDEP2 upon transduction with the empty vector (-) or with the COUP-TFII expressing vector (+) in proliferation and differentiation conditions. Expression levels are expressed relative to GAPDH and in relative ratios ($n \geq 3$; *=$p \leq 0.05$; **=$p \leq 0.01$; ***=$p \leq 0.001$). **B)** Representative Western blots showing the increase of γ-globin and the parallel decrease of β-globin at the protein level in HUDEP2 cells expressing Coup-TFII (total protein extracts -TE- 48 hours of differentiation). Given the abundance of β-globin, different exposures are shown for optimal visualization of the bands. **C)** Jaspar matrix of DNA binding sites recognized by COUP-TFII and BCL11A-XL. **D)** EMSA: Nuclear extracts from COS7 cells transfected either with a BCL11A-XL-myc or a COUP-TFII-Flag vector were incubated with a probe corresponding to the COUP-TFII target region on the ApoAI enhancer(20), containing a double COUP-TFII consensus site. BCL11A-XL and COUP-TFII were univocally identified by using α-myc (Ab32 Abcam) and α-Flag (F7425 Sigma-Aldrich) antibodies. Asterisks indicate bands likely due to the binding of two molecules of the same protein. **E)** Venn diagram showing overlapping BCL11A-XL and COUP-TFII peaks in HUDEP2 cells**. F)** Signal intensity plot summarizing the replicate average signal intensities across different genomic regions for common and specific COUP-TFII- and BCL11A-XL-peaks in HUDEP2. COUPTFII (left) and BCL11A-XL (right). Two replicates per each factor were considered for the analysis. **G)** List of DEGs following TF perturbation that are most similar to the list of genes associated with COUP-TFII peaks (HUDEP1 and HUDEP2 merged, (https://maayanlab.cloud/Enrichr/enrich?dataset=bfd73c13b56ba7bbecd7a75c3e725f5c). **H)** IGV visualization for COUP-TFII and BCL11A-XL (data from Liu et al.(19)) CUT&RUN profiles at the β-globin locus. The arrow marks an unspecific CUT&RUN artifact, also generated by the anti-Flag

control antibody, likely caused by the extreme accessibility of the region in erythroid cells (30, 31). See Methods for data processing for the comparison of the two data sets.

Figure 3: In depth analysis of COUP-TFII binding to the adult δ and β promoters, within a region target of deletional HPFH. A) IGV visualization for COUP-TFII CUT&RUN profile at the β- globin locus in HUDEP2 cells considering 3 out of 4 peaks, obtained with two independent antibodies. The arrow marks an unspecific CUT&RUN artifact. The plot is superimposable to that obtained with the previous analysis in Figure2H. **B)** Footprints at the δ and β promoters. **C)** Alignment of COUP-TFII peaks with some overlapping naturally occurring deletional HPFH within the β-locus. Deletions involving both δ and β COUP-TFII-bound promoters (in red) are amongst the ones associated with the highest γ-globin levels. HbF levels are indicated beside each type of deletion (32). **D-E)** HUDEP1 cells analysis: COUP-TFII occupancy mapped by CUT&RUN (D) and RTqPCR on globins genes (E) Expression levels are expressed relative to GAPDH and in relative ratios (n≥3; *=p≤0.05; **=p≤0.01;***=p≤0.001).

Figure 4: COUP-TFII binds to the *BCL11A* locus and binds to and activates LIN28B

A) In HUDEP2 cells, COUP-TFII binds to the *BCL11A* locus. Left panels: IGV visualization of CUT&RUN tracks at the *BCL11A* +55region. Middle panel: RT-qPCR for BCL11A-XL in HUDEP2 cells upon transduction with the empty vector (-) or with the COUP-TFII expressing vector (+) in proliferation and differentiation conditions. Expression levels are relative to GAPDH (n≥3; **=p≤0.01; ***=p≤0.001). Right panel: Western blot analysis showing BCL11A-XL protein upon Coup-TFII expression in differentiation conditions.

B) In HUDEP1 cells, COUP-TFII binds to and activates LIN28B. The same analysis as in A was applied to Lin28B. Western blot was performed in cells under proliferation conditions. **C)** Proposed model for the COUP-TFII role in controlling the hemoglobin fetal-to-adult transition. In fetal-like HUDEP1 cells, γ-globin is expressed at very high levels. In these cells, COUP-TFII binds to the LCR, increasing ε but -not detectably- γ transcription levels. In addition to interacting with the β-locus, COUP-TFII binds to and activates the transcription of *LIN28B*, a post-transcriptional repressor of BCL11A-XL(11). Instead, SOX6 contributes to the silencing of Lin28B(29) and cooperates with BCL11A-XL(28). In HUDEP2, where the full set of γ-globin inhibitors (including BCL11A-XL) is present, both γ-globin and LIN28B expression are switched off and β-globin is actively transcribed. In these cells, COUP-TFII occupies the δ and β promoters. Overall, COUP-TFII expression results in activation of embryo/fetal genes and in reduction of β. Our working model highlights COUP-TFII multiple contributions to

establishing an environment favorable to the expression of γ-globin genes and proposes a molecular mechanism to explain its ability to relieve γ-globin repression in adult cells.

Figure 1

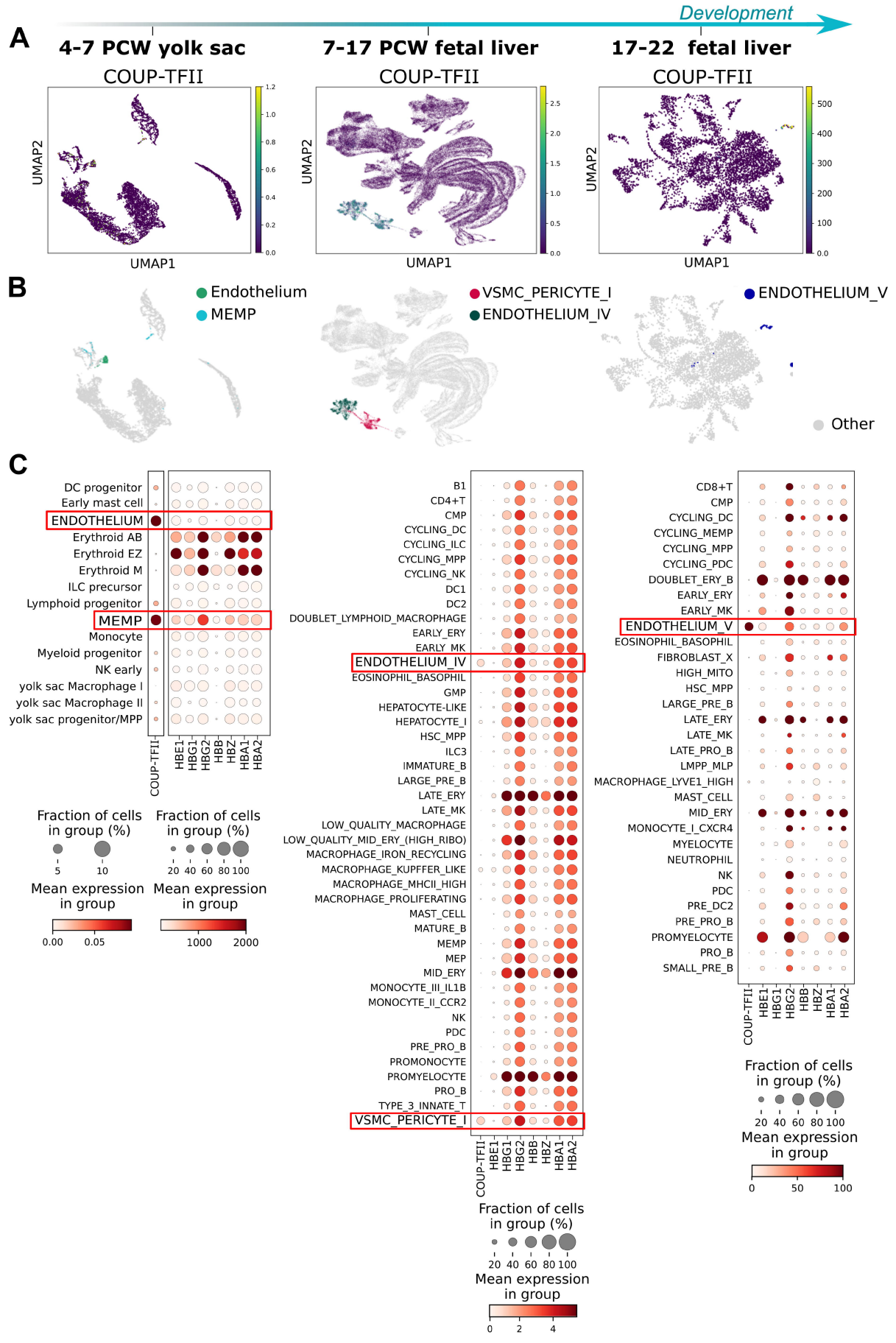
A
Development
4-7 PCW yolk sac
7-17 PCW fetal liver
17-22 fetal liver
COUP-TFII
UMAP1
UMAP2
B
Endothelium
MEMP
VSMC_PERICYTE_I
ENDOTHELIUM_IV
ENDOTHELIUM_V
Other
C
DC progenitor
Early mast cell
ENDOTHELIUM
Erythroid AB
Erythroid EZ
Erythroid M
ILC precursor
Lymphoid progenitor
MEMP
Monocyte
Myeloid progenitor
NK early
yolk sac Macrophage I
yolk sac Macrophage II
yolk sac progenitor/MPP
COUP-TFII
HBE1
HBG1
HBG2
HBB
HBZ
HBA1
HBA2
Fraction of cells in group (%)
Mean expression in group
B1
CD4+T
CMP
CYCLING_DC
CYCLING_ILC
CYCLING_MPP
CYCLING_NK
DC1
DC2
DOUBLET_LYMPHOID_MACROPHAGE
EARLY_ERY
EARLY_MK
ENDOTHELIUM_IV
EOSINOPHIL_BASOPHIL
GMP
HEPATOCYTE-LIKE
HEPATOCYTE_I
HSC_MPP
ILC3
IMMATURE_B
LARGE_PRE_B
LATE_ERY
LATE_MK
LOW_QUALITY_MACROPHAGE
LOW_QUALITY_MID_ERY_(HIGH_RIBO)
MACROPHAGE_IRON_RECYCLING
MACROPHAGE_KUPFFER_LIKE
MACROPHAGE_MHCII_HIGH
MACROPHAGE_PROLIFERATING
MAST_CELL
MATURE_B
MEMP
MEP
MID_ERY
MONOCYTE_III_IL1B
MONOCYTE_II_CCR2
NK
PDC
PRE_PRO_B
PROMONOCYTE
PROMYELOCYTE
PRO_B
TYPE_3_INNATE_T
VSMC_PERICYTE_I
CD8+T
CMP
CYCLING_DC
CYCLING_MEMP
CYCLING_MPP
CYCLING_PDC
DOUBLET_ERY_B
EARLY_ERY
EARLY_MK
ENDOTHELIUM_V
EOSINOPHIL_BASOPHIL
FIBROBLAST_X
HIGH_MITO
HSC_MPP
LARGE_PRE_B
LATE_ERY
LATE_MK
LATE_PRO_B
LMPP_MLP
MACROPHAGE_LYVE1_HIGH
MAST_CELL
MID_ERY
MONOCYTE_I_CXCR4
MYELOCYTE
NEUTROPHIL
NK
PDC
PRE_DC2
PRE_PRO_B
PROMYELOCYTE
PRO_B
SMALL_PRE_B

Figure 2

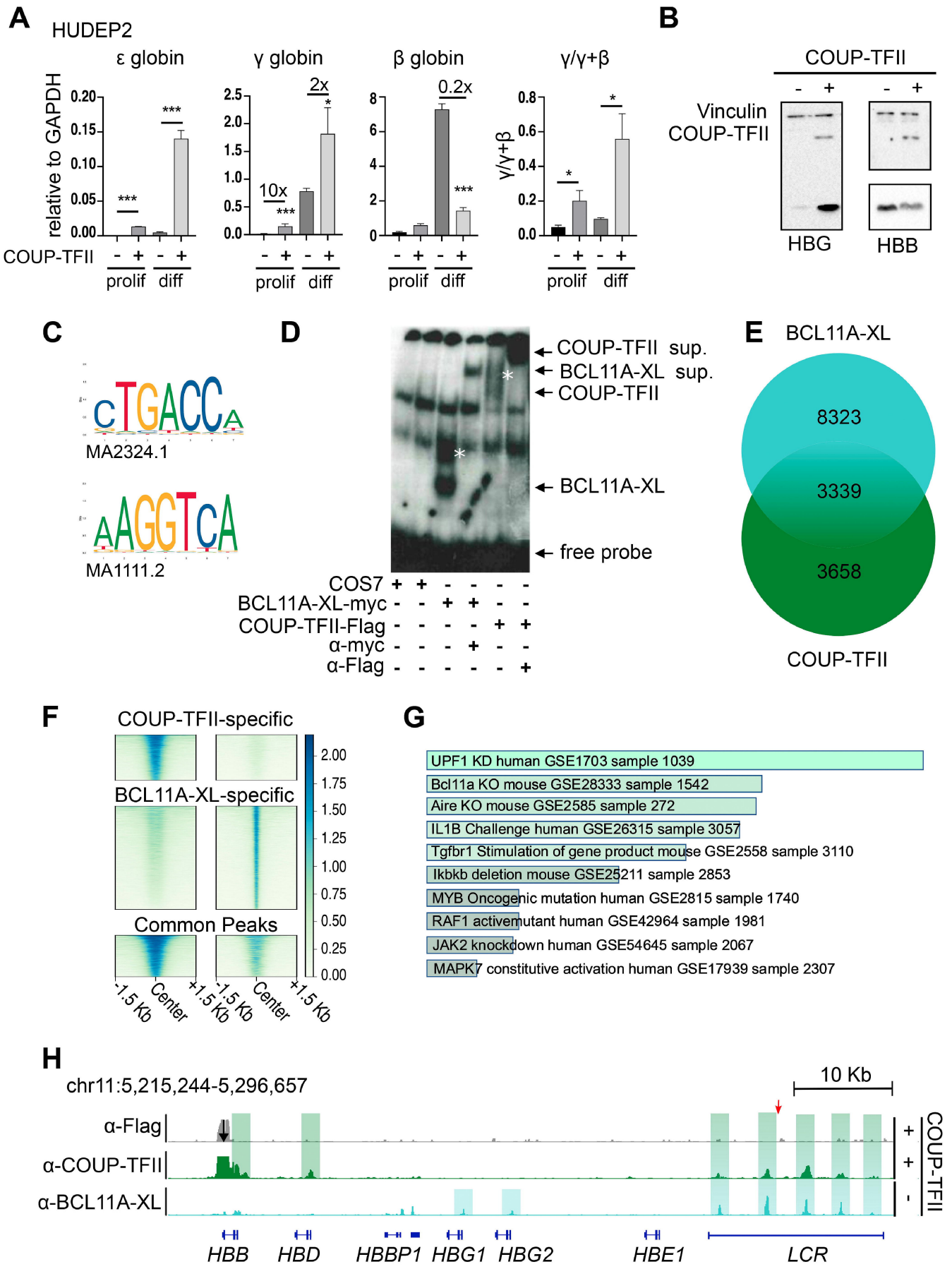
A
HUDEP2
ε globin
γ globin
β globin
γ/γ+β
relative to GAPDH
COUP-TFII
prolif
diff
2x
10x
0.2x
B
COUP-TFII
Vinculin
COUP-TFII
HBG
HBB
C
MA2324.1
MA1111.2
D
COUP-TFII sup.
BCL11A-XL sup.
COUP-TFII
BCL11A-XL
free probe
COS7
BCL11A-XL-myc
COUP-TFII-Flag
α-myc
α-Flag
E
BCL11A-XL
8323
3339
3658
COUP-TFII
F
COUP-TFII-specific
BCL11A-XL-specific
Common Peaks
-1.5 Kb
Center
+1.5 Kb
G
UPF1 KD human GSE1703 sample 1039
Bcl11a KO mouse GSE28333 sample 1542
Aire KO mouse GSE2585 sample 272
IL1B Challenge human GSE26315 sample 3057
Tgfbr1 Stimulation of gene product mouse GSE2558 sample 3110
Ikbkb deletion mouse GSE25211 sample 2853
MYB Oncogenic mutation human GSE2815 sample 1740
RAF1 activemutant human GSE42964 sample 1981
JAK2 knockdown human GSE54645 sample 2067
MAPK7 constitutive activation human GSE17939 sample 2307
H
chr11:5,215,244-5,296,657
10 Kb
α-Flag
α-COUP-TFII
α-BCL11A-XL
COUP-TFII
HBB
HBD
HBBP1
HBG1
HBG2
HBE1
LCR

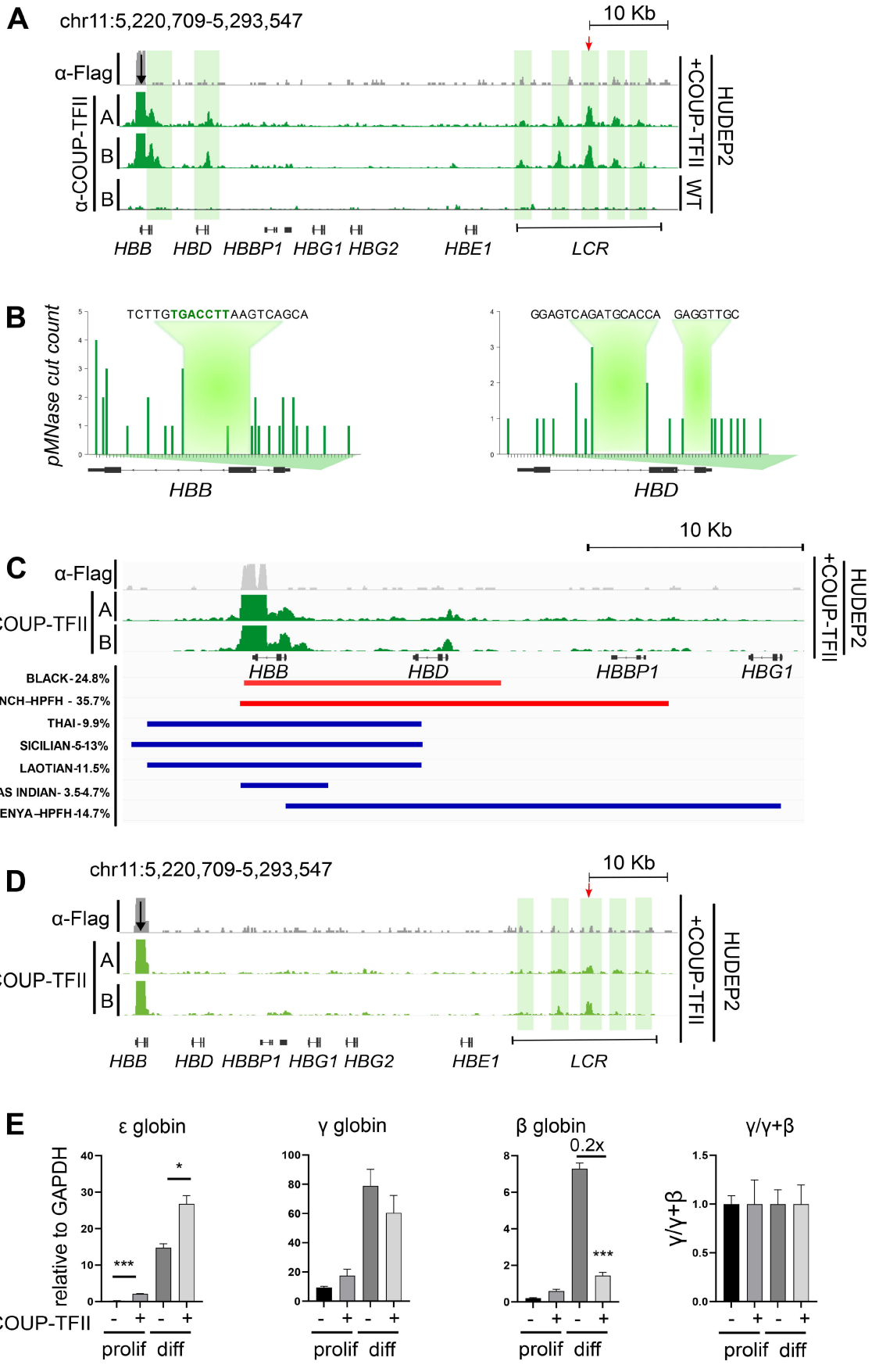

Figure 3 *Frigo et al.*

Figure 4 *Frigo et al.*

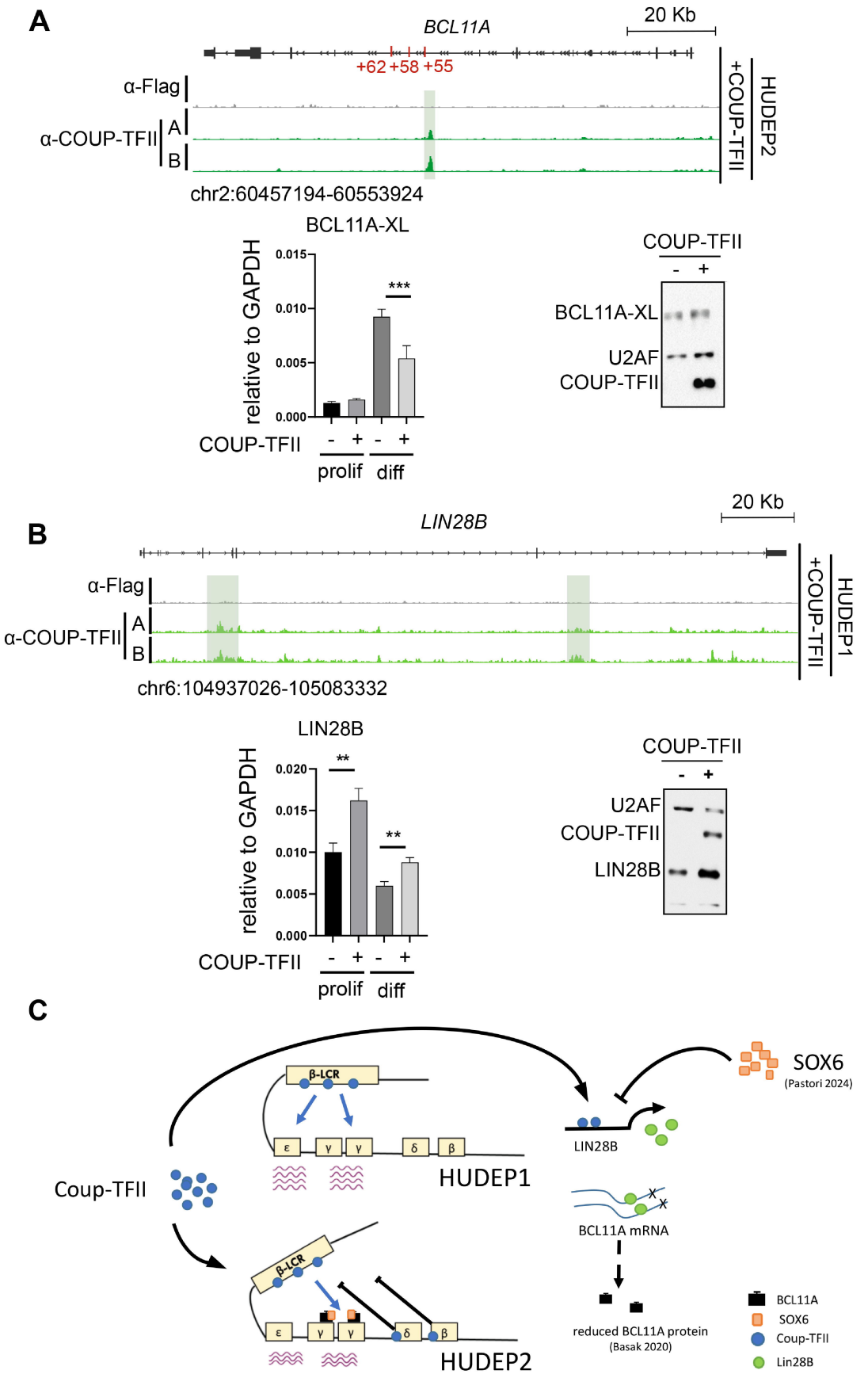

COUP-TFII regulates hemoglobin switching by activating the BCL11A-XL repressor Lin28B and directly binding δ and β globin promoters in fetal versus adult erythroid cells *Carlotta Frigo et. al.*

SUPPLEMENTAL FIGURES

SUPPLEMENTAL FIGURE 1

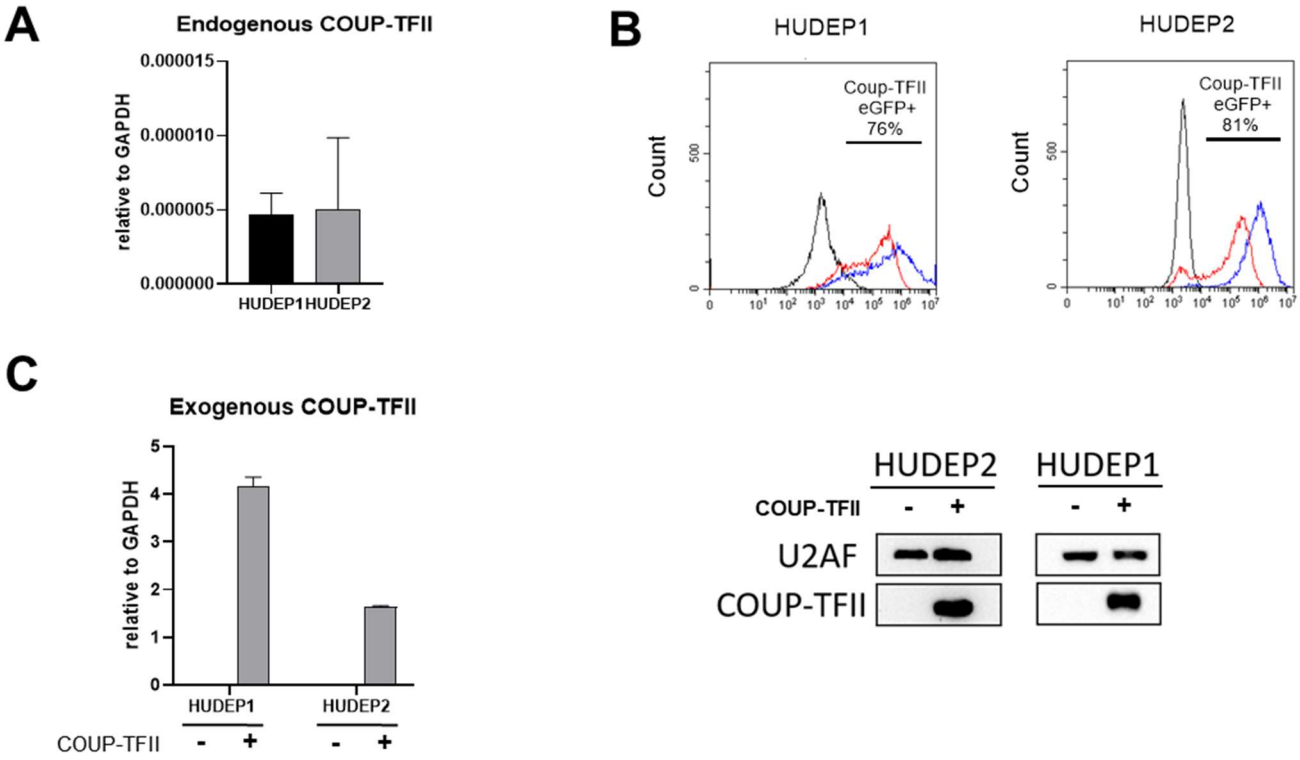

A) HUDEP1 and HUDEP2 cells do not express COUP-TFII. Endogenous COUP-TFII expression level evaluated by RTqPCR relative to GAPDH. **B) Representative transduction experiment.** The efficiency of HUDEP1 and HUDEP2 transduction was evaluated by Flow cytometry as percentage of GFP+ cells, since the expression vector contains a bicistronic Coup-TFII-IRES-GFP cassette. x axis: Mean Fluorescence Intensity; y axis: cell count. Gray: un-transduced cells. Blue: GFP^+ cells infected with the Empty Vector (-). Red: GFP^+ cells infected with the Coup-TFII-expressing vector (+). **C)** Corresponding exogenous Coup-TFII RNA (left) and protein (right) expression.

SUPPLEMENTAL FIGURE 2

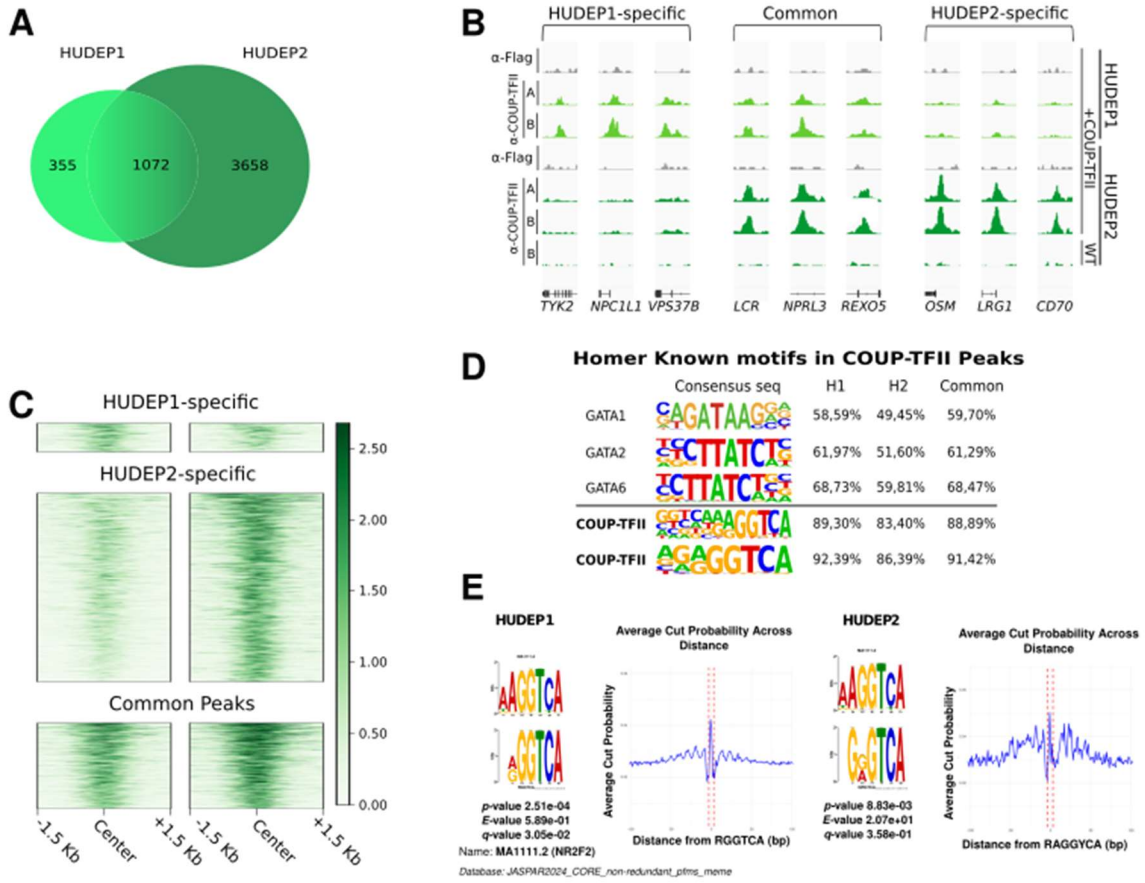

COUP-TFII genomic occupancy in HUDEP1 and HUDEP2 cells. A) Venn diagram showing the overlap between COUP-TFII high-confidence peaks called in HUDEP1 and HUDEP2. **B)** IGV representation of three examples of COUP-TFII peaks in each category: HUDEP1-specific, common, HUDEP2-specific. Antibodies, cell lines, and treatment are indicated. Two anti-COUP-TFII antibodies, A (α-COUP-TFII A: ABIN6928040) and B (α-COUP-TFII B: ab41859) were used, each of them in two replicates and we considered high-confidence peaks those detected in at least 3 out of 4 replicates. The negative controls include an α-Flag antibody in COUP-TFII expressing cell lines and COUP-TFII antibody B (α-COUP-TFII B) in un-transduced HUDEP2 (WT). +COUP-TFII: cells transduced with the COUP-TFII expressing vector. **C)** Signal intensity plots summarizing the replicate average signal intensities across different genomic regions for common and unique COUP-TFII peaks in HUDEP1 (left) and HUDEP2 (right). **D)** Known motifs discovery by HOMER analysis within COUP-TFII peaks. Each motif, its likely binding factor and its frequency in HUDEP1 (H1), HUDEP2 (H2), or in shared peaks (common) are indicated. **E)** *De novo* motifs (corresponding to the COUP-TFII Jaspar Matrix MA1111.2) identified genome-wide by COUP-TFII antibodies in CUT&RUN experiments in HUDEP1 (left) and HUDEP2 (right). Average cut probability across the COUP-TFII site is plotted in the corresponding right panels.

SUPPLEMENTAL FIGURE 3

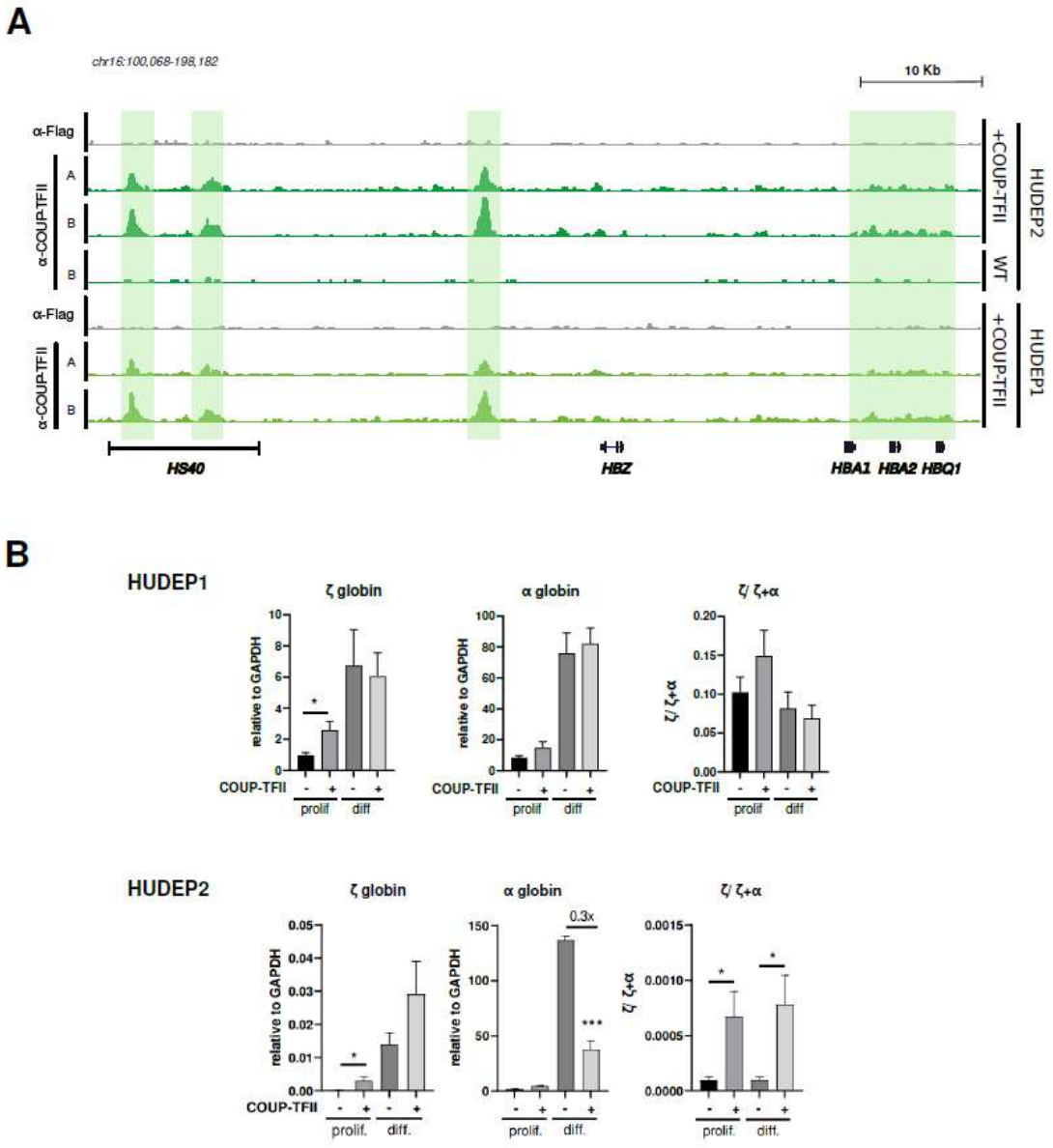

α-globin locus analysis. A) COUP-TFII CUT&RUN profile at the α-locus in HUDEP1 and HUDEP2 visualized in IGV. **B)** RT-qPCR analysis of mRNA levels for the indicated globin genes in HUDEP1 (upper panel) and HUDEP2 (lower panel) upon transduction with the empty vector (-) or with the COUP-TFII expressing vector (+) in proliferation and differentiation conditions. Expression levels are expressed relative to GAPDH and in relative ratios (n≥3; *=p≤0.05; **=p≤0.01; ***=p≤0.001)

SUPPLEMENTAL METHODS

Library preparation

Library preparation was performed using the KAPA Hyper Prep Kit for Illumina platforms (Cat. #KK8504, KAPA Biosystems) according to the manufacturer's guidelines with the following modifications. End repair and A-tailing was performed with 0.4x reactions with 20 µl of purified DNA. The thermocycler conditions were set to 12 °C for 15 min, 37 °C for 15 min and 58 °C for 25 min to prevent thermal degradation of the shortest fragments. Adapter ligation was done with 0.4x reactions. KAPA Dual Indexed adapters were used at 0.15 µM. A post-ligation clean-up was performed with Mag-Bind TotalPure NGS beads at 1.2x. Resuspension was done in 10 mM Tris-HCl pH 8.0. Library amplification was performed with 0.5x reactions. The thermocycler was set with the following conditions: initial denaturation at 98 °C for 45 sec, denaturation at 98 °C for 15 sec, annealing/elongation at 60 °C for 10 sec, final extension at 72 °C for 1 min, hold at 4 °C, with 13 cycles. After amplification, a post-amplification cleanup was performed with 1.2x beads. Libraries were then run on an E-Gel EX 2% agarose gel (Cat. #G402022, Invitrogen) for 10 min using the E-Gel Power Snap Electrophoresis System (Invitrogen). Bands of interest between 150 and 500 bp were cut out and purified using the QIAquick Gel Extraction Kit (Cat. #28706, QIAGEN) according to manufacturer's instructions. Libraries were quantified with the Qubit (Thermo Scientific) using their high sensitivity DNA kit (Cat #Q32854, Thermo Scientific), pooled and sequenced 36 bp pair-end on the NextSeq 550 (Illumina) using the Illumina NextSeq 500/550 High Output Kit v2.5 (75 cycles) (Cat. #20024906, Illumina). The CUT&RUN datasets (raw and processed files) have been deposited at ArrayExpress (https://www.ebi.ac.uk/arrayexpress/) under accession number E-MTAB-14720.

Cell line	Condition	Antibody
HUDEP1	COUPTFII vector	Flag F7425
HUDEP1	COUPTFII vector	COUPTFII A ABIN6928040 (Lot HD09MA0327-B)
HUDEP1	COUPTFII vector	COUPTFII B ab41859
HUDEP2	WT	COUPTFII B ab41859
HUDEP2	COUPTFII vector	Flag F7425
HUDEP2	COUPTFII vector	COUPTFII A ABIN6928040 (Lot HD09MA0327-B)
HUDEP2	COUPTFII vector	COUPTFII B ab41859

Data Analysis

Trimming was performed using bbmap bbduk(1) (version 39.0) removing adapters, artifacts, poly AT, G and C repeats. Reads were aligned to the hg38 genome with bowtie (2) (version 1.3.1) using options -v 0 -m 1 -X 500. Samtools(3) (version 1.6) view, fixmate, markdup and sort were used to create bam files, mark and remove duplicates, and sort bam files. Mitochondrial reads were removed together with the problematic of problematic regions as described in ref. (4). Individual track bedgraphs were created using bedtools(5) (version 2.30.0) genomecov on pair-end mode. Normalized signal per million reads tracks for visualization were created by using the –SPRM function of macs2(6) (version 2.2.6) for each replicate with the options -f BAMPE –SPMR and –bdg. After normalization 2 replicate per Antibody were averaged out using the bigwigAverage function of Deeptools(7) (version 3.5.2). Peaks were called using SEACR(8) (version 1.3) against the corresponding negative control using the options “norm, stringent”. Venn diagrams and overlap peak sets were created using Intervene(9) (version 0.6.5). Motif analysis was done using Homer(10) (version 4.11) findMotifsGenome to find motifs in the hg38 genome using -size given. Peak set gene annotation was done using GREAT(11) (version 4.0.4) with default parameters. Signal intensity plots were created using the Deeptools(7) (version 3.5.2) functions computeMatrix reference-point, with the parameters -H chromosome length, -referencePoint center, -a 1500, -b 1500 and plotHeatmap. Footprint analysis: to identify potentially enriched sequences within the CUT&RUN peaks, we employed MEME Suite(18) (version 5.5.6) for de novo motif discovery. Sequences spanning from -100 bp to +100 bp relative to the intermediate positions of 1000 randomly selected peaks were analyzed. The top 10 enriched motifs were extracted using DREME (-dreme-m 10). Motifs were annotated using tomtom with the JASPAR database. The sequences containing the motifs where then extracted using FIMO and the cut frequency matrix was computed via CUT-RUNTools-2.0 package(12) with make_cut_matrix (version 0.1.6). The variation in cut probabilities relative to the distance from the motif center was visualized using R (version 4.3.3). Single locus footprinting analysis was performed adapting get_cuts_single_locus.sh, also from CUT-RUNTools-2.0 package.

Comparison between the CUT&RUN occupancy of BCL11A-XL and COUP-TFII.

For the comparison with BCL11A-XL we downloaded raw data from Liu N. et al. (13) (accession number GEO: GSE104676) and we aligned them with Bowtie2, as described in the paper with the following modification: all tracks were filtered the suspect of problematic regions as

described in ref.(4). We selected tracks for 2 BCL11A-XL replicates in WT and to have a fair comparison we realigned our data (only antibody B) together with the BCL11A-XL dataset.

Sample/Dataset	Cell line and condition	Antibody
SRR6144299	HUDEP2	BCL11A
SRR6144304	HUDEP2	BCL11A

For visualization purposes the 2 replicate per condition were averaged out using the bigwigAverage function of Deeptools (Ramírez et al., version 3.5.2).

1. Bushnell B, Rood J, Singer E. BBMerge - Accurate paired shotgun read merging via overlap. PloS one. 2017;12(10):e0185056.
2. Langmead B, Trapnell C, Pop M, Salzberg SL. Ultrafast and memory-efficient alignment of short DNA sequences to the human genome. Genome Biol. 2009;10(3):R25.
3. Li H, Handsaker B, Wysoker A, Fennell T, Ruan J, Homer N, et al. The Sequence Alignment/Map format and SAMtools. Bioinformatics. 2009;25(16):2078-9.
4. Nordin A, Zambanini G, Pagella P, Cantu C. The CUT&RUN suspect list of problematic regions of the genome. Genome Biol. 2023;24(1):185.
5. Quinlan AR, Hall IM. BEDTools: a flexible suite of utilities for comparing genomic features. Bioinformatics. 2010;26(6):841-2.
6. Zhang Y, Liu T, Meyer CA, Eeckhoute J, Johnson DS, Bernstein BE, et al. Model-based analysis of ChIP-Seq (MACS). Genome Biol. 2008;9(9):R137.
7. Ramirez F, Ryan DP, Gruning B, Bhardwaj V, Kilpert F, Richter AS, et al. deepTools2: a next generation web server for deep-sequencing data analysis. Nucleic Acids Res. 2016;44(W1):W160-5.
8. Meers MP, Tenenbaum D, Henikoff S. Peak calling by Sparse Enrichment Analysis for CUT&RUN chromatin profiling. Epigenetics Chromatin. 2019;12(1):42.
9. Khan A, Mathelier A. Intervene: a tool for intersection and visualization of multiple gene or genomic region sets. BMC Bioinformatics. 2017;18(1):287.
10. Heinz S, Benner C, Spann N, Bertolino E, Lin YC, Laslo P, et al. Simple combinations of lineage-determining transcription factors prime cis-regulatory elements required for macrophage and B cell identities. Mol Cell. 2010;38(4):576-89.
11. McLean CY, Bristor D, Hiller M, Clarke SL, Schaar BT, Lowe CB, et al. GREAT improves functional interpretation of cis-regulatory regions. Nat Biotechnol. 2010;28(5):495-501.
12. Yu F, Sankaran VG, Yuan GC. CUT&RUNTools 2.0: a pipeline for single-cell and bulk-level CUT&RUN and CUT&Tag data analysis. Bioinformatics. 2021;38(1):252-4.
13. Liu N, Hargreaves VV, Zhu Q, Kurland JV, Hong J, Kim W, et al. Direct Promoter Repression by BCL11A Controls the Fetal to Adult Hemoglobin Switch. Cell. 2018;173(2):430-42 e17.